MATHEMATICAL MODEL OF THE DEFORMATION AND FRACTURE OF SOLID FUEL IN SHOCK LOADING

A. B. Kiselev and M. V. Yumashev

UDC 539.3

Solid fuels are used as the propellants for many types of rockets. The structure of many such materials is nonuniform due to the combination of melted crystalline oxidants and a polymer matrix, with the latter accounting for a large percentage of the weight of the fuel. The technology used to make solid fuels does not make it possible to completely eliminate scattered micropores, which may be one reason for poor fuel performance. Pores may also be present as a result of long storage of the fuel, since slow chemical reactions take place in the fuel under normal conditions. These reactions result in the formation of gas in the material – a process which in particular leads to the development of microscopic cavities. In addition, accidents which might occur during transport of the fuel can involve shock loading of the grain and the consequent formation of cracks and other discontinuities in the fuel. The behavior of such discontinuities is of great interest, since they influence the dominant combustion path and may disturb the equilibrium of the rocket in flight or even lead to explosion of the system [1]. Among the most important problems facing researchers are predicting the behavior of solid fuels under shock loading and evaluating the level of dynamic loading that is permissible from the viewpoint of maintaining the integrity of the structure and minimizing the danger of fire and explosion.

In the present study, we model solid fuel as a porous thermoelastic medium. As such the model is among the class of models presently being actively developed on the basis of thermodynamic principles of continuum mechanics to describe media with internal state parameters. The principles underlying the phenomenological description of such media were presented in [2-4] while [5-10] discussed the main trends in this area and presented a bibliography of relevant publications. The model being constructed here is closest to the model presented in [11] to describe a thermoelastoplastic medium being plastically deformed.

1. Model of the Medium. Following [11], we can obtain the system of governing equations of the proposed model if we replace one of the internal state parameters of the model in [11] (damage content ω) by the porosity parameter α ($0 \leq \alpha < 1$). This parameter represents the volume content of micropores (cavities in the fuel). In this case, the governing equations are written in the form:

$$\begin{aligned}
&\dot{\sigma}' = K_0\left(\dot{\varepsilon}_{kk} - \alpha_V \dot{T} - \frac{A}{3}\dot{\alpha}\frac{\partial \dot{\alpha}}{\partial \sigma}\right),\\
&(\tau_{ij}')^{\nabla} + \lambda \tau_{ij}' = 2\mu_0 \dot{e}_{ij}, \quad \tau_{ij}'\tau_{ij}' \leqslant \frac{2}{3}Y^2,\\
&\rho c_\sigma \dot{T} + \alpha_V \dot{\sigma} T = \tau_{ij}\dot{\varepsilon}_{ij}^p + A\dot{\alpha}^2 - \operatorname{div} \mathbf{q},\\
&\tau_{ij} = S_{ij} + \Gamma \varepsilon_{ij}^p, \quad \tau_{ij}' = \frac{\tau_{ij}}{1-\alpha}, \quad \sigma' = \frac{\sigma}{1-\alpha}.
\end{aligned} \tag{1.1}$$

Here, σ_{ij} are components of the stress tensor resolved into two mutually orthogonal tensors: the spherical tensor $\sigma\delta_{ij} = \sigma_{kk}\delta_{ij}/3$ and the deviator S_{ij}: $\sigma_{ij} = \sigma\delta_{ij} + S_{ij}$; ε_{ij}, $\varepsilon^e{}_{ij}$, $\varepsilon^P{}_{ij}$ are components of the tensors of the total, elastic, and plastic strains, respectively ($\varepsilon_{ij} = \varepsilon^e{}_{ij} + \varepsilon^P{}_{ij}$, $\varepsilon^P{}_{kk} = 0$); e_{ij} are components of the deviator of the strain tensor; T is absolute temperature; q is heat flux; K_0 and μ_0 are the compressive bulk modulus and shear modulus of the solid material ($\alpha = 0$); α_V is the coefficient of cubicle expansion; Y is the yield point; c_σ is heat capacity at constant stress; A and Γ are characteristics of the material. A dot above a given symbol denotes the material derivative with respect to time, while the symbol ∇ denotes the Jaumann time derivative of the components of the tensor.

Equations (1.1) were obtained on the basis of a standard thermodynamic analysis with the assumption that the material behaves in an elastoplastic manner. The following simplifying assumptions were also made in deriving the equations.

Moscow. Translated from Prikladnaya Mekhanika i Tekhnicheskaya Fizika, No. 6, pp. 126-134, November-December, 1992. Original article submitted November 25, 1991.

0021-8944/92/3306-0885$12.50

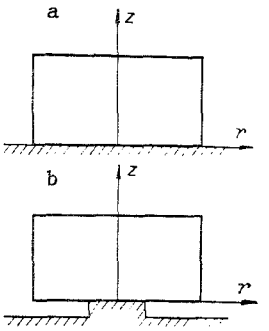

Fig. 1

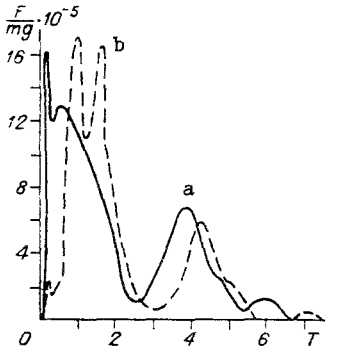

Fig. 2

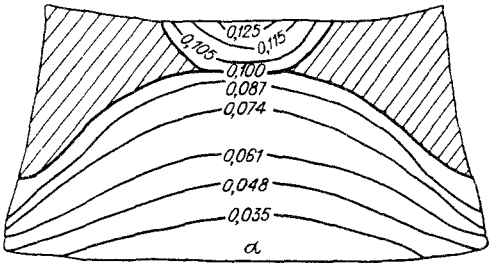

Fig. 3

A. The elastic strain are small: $\varepsilon^e_{ij}\varepsilon^e_{ij} \ll 1$.

B. The free energy F_p, being a function of the independent variables ε^e_{ij}, ε^p_{ij}, α and T, can be represented as the sum of two terms

$$F = F_1(\varepsilon^e_{ij}, \alpha, T) + F_2(\varepsilon^p_{ij}, \alpha, T).$$

This hypothesis is equivalent to assuming that the cumulative strains do not change the elastic properties of the material [11].

C. The dissipation function $d \geq 0$ can be described as the sum of three nonnegative terms:

$$d = d_m + d_s + d_T, \quad d_m = \left(\sigma_{ij} - \rho\frac{\partial F}{\partial \varepsilon^p_{ij}}\right)\dot{\varepsilon}^p_{ij} \geqslant 0,$$

$$d_s = -\rho\frac{\partial F}{\partial \alpha}\dot{\alpha} \geqslant 0, \quad d_T = -\frac{\mathbf{q}\,\mathrm{grad}\,T}{T} \geqslant 0$$

(d_m is the capacity for mechanical dissipation; d_s is the capacity for energy dissipation due to the evolution of scattered micropores; d_T is the capacity for heat dissipation). We also introduced the notation

$$\tau_{ij} = \sigma_{ij} - \rho\partial F/\partial\varepsilon^p_{ij}.$$

The tensor τ_{ij} is referred to as the tensor of the "active" stresses. It is evident from (1.1) that if free energy F depends on the plastic strains ε^p_{ij}, then the energy dissipation process is determined by the "active" stresses τ_{ij} rather than by the true stresses σ_{ij}. The introduction of the plastic strain ε^p_{ij} into free energy F makes it possible to account for strain anisotropy of the material which is manifest with plastic deformation.

We also assume that

$$-\rho\frac{\partial F}{\partial \varepsilon^p_{ij}} = \Gamma\varepsilon^p_{ij}, \quad -\rho\frac{\partial F}{\partial \alpha} = A\dot{\alpha}$$

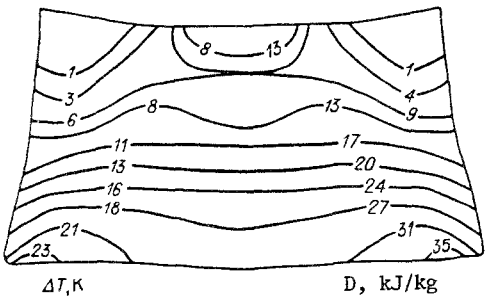

Fig. 4

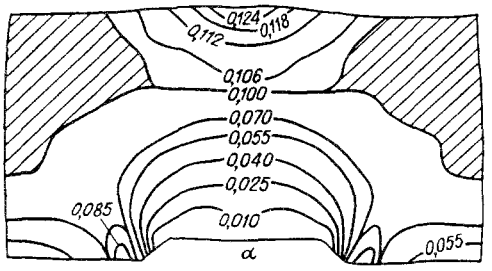

Fig. 5

($\Gamma \geq 0$, $A \geq 0$ are parameters of the material). When A = const, the second of these relations is a corollary of the Onsager theory [12].

D. The moduli K and μ of the porous material depend on porosity α:

$$K = K_0(1-\alpha), \quad \mu = \mu_0(1-\alpha).$$

We take the following as the kinetic equation for the porosity parameter α to close system (1.1):

$$\frac{\dot{\alpha}}{\alpha} = \frac{\sigma - \sigma^+}{4\eta} H(\sigma - \sigma^+) + \frac{\sigma - \sigma^-}{4\eta} H(\sigma^- - \sigma). \tag{1.2}$$

Here,

$$\sigma^+ = -\frac{2}{3} Y \ln \alpha - p_0 \left(\frac{\alpha_0}{\alpha}\right)^k, \quad \sigma^- = \frac{2}{3} Y \ln \alpha - p_0 \left(\frac{\alpha_0}{\alpha}\right)^k \tag{1.3}$$

(η is the absolute viscosity of the material; α_0 is initial porosity). Equations (1.2)-(1.3) were obtained from the solution of the problem of the dynamics of a single spherical pore of internal radius a and external radius b in a viscoplastic incompressible material when $\alpha = a^3/b^3$ [13-16]. Here, we also approximately accounted for the pressure of the gas in the pore and on its inside surface, as well as the change in the radius of the cavity (with allowance for the fact that the pressure in the gas cavity instantaneously reacts to a change in the radius of the cavity). The process of compression of the gas was assumed to be adiabatic [17]. In (1.3), p_0 is the initial pressure of the gas in the pore; k is the adiabatic exponent.

Model (1.1)-(1.3) generalizes the Prandtl–Reuss model of elastoplastic flow with the von Mises yield criterion and accounts for the anisotropy of plastic deformation ($\Gamma \neq 0$), the presence of micropores in the material, the growth of these pores in rarefaction waves and their collapse in compression waves, the mutual effect of the porosity and stress state of the material, and temperature effects. The model does not contain an explicit dependence on strain rate, since it is to be used in high-rate loading processes in which viscous effects not connected with the inertia of the pores can be ignored. In fact, the characteristic time of the problem $t_3 = L/c_0$ is much greater than the relaxation time $\tau = \eta/\mu$, which is in turn comparable to the characteristic time in the problem of the dynamics of an individual pore $t_s = d/c_0$ (L is the characteristic dimension of the body, c_0 is the speed of sound in the material, and d is the diameter of the pore).

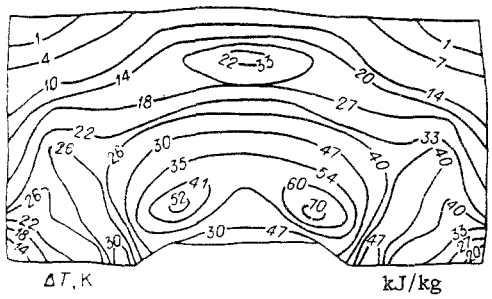

Fig. 6

The yield point Y and shear modulus μ depend on temperature, pressure, and other state parameters. We assume that this dependence can be described by the Steinberg–Wynan model [18]:

$$Y = Y_0(1+\beta\varepsilon_{in}^p)^n\left(1 - b\sigma\left(\frac{\rho_0}{\rho}\right)^{1/3} - h(T-T_0)\right),$$

$$Y_0(1+\beta\varepsilon_{in}^p)^n \leqslant Y_{max},\ Y_0 = 0 \quad \text{at} \quad T > T_m,$$

$$T_m = T_{m0}\left(\frac{\rho_0}{\rho}\right)^{2/3}\exp\left(2\gamma_0\left(1-\frac{\rho_0}{\rho}\right)\right),$$

$$\mu_0 = \mu_{00}\left(1 - b\sigma\left(\frac{\rho_0}{\rho}\right)^{1/3} - h(T-T_0)\right)$$

(ε^p_{in} is the intensity of the plastic strains; Y_0, Y_{max}, h, μ_{00}, β, n, b, γ_0 are material constants).

2. Failure Criterion. As the criterion of failure of the solid fuel (the nucleation of cracks – a new free surface in the material), we take the condition for the attainment of the limiting value D_* by unit (per unit of mass) dissipation [11, 19]:

$$D = \int_0^{t_*} \frac{1}{\rho} d\, dt = D_*. \tag{2.1}$$

Here, t_* is the time to failure; D_* is a material constant which is determined experimentally; d is the dissipation function. For the given model, this function has the form

$$d = \tau_{ij}\dot{\varepsilon}^p_{ij} + A\dot{\alpha}^2 - \frac{q\,\mathrm{grad}\,T}{T}. \tag{2.2}$$

Following the classification in [20], criterion (2.1) can be considered an entropy-based failure criterion ($d = \rho\gamma$, where γ is the derivative of entropy [11]). In principle, such a failure criterion makes it possible to describe the process of failure by two mechanisms. The first involves the growth and coalescence of micropores, such as occurs in the case of failure by cleavage in rarefaction waves [in this case, along with the capacity for mechanical dissipation $d_m = \tau_{ij}\varepsilon^p_{ij}$, the capacity for energy dissipation due to micropore growth $d_S = A\dot{\alpha}^2$ makes the main contribution to (2.1)-(2.2)]. In the case of tensile failure, the failure process may be facilitated by prior shock compression of the material. Such compression heats the material, making it more "compliant" and causing tensile fracture to occur more rapidly. The second mechanism involves failure in shear. This occurs (for example) when a foreign object with a planar leading edge is introduced into the grain. In this case, narrow zones of intensive adiabatic shear develop at stress concentration sites in the material about the periphery of the foreign body. The work done in plastic deformation is almost entirely converted to heat and, due to the high local strain rates, there is not enough time for this heat to propogate a substantial distance from the zones of developed plastic strain. As a result, the temperature in these zones rises and large temperature gradients are formed. The latter in turn results in additional plastic flow and further concentration of local plastic strains, ultimately leading to the motion of "plugs" in the material and – in some cases – to the ejection of these plugs from the grain. In the case of shear failure, the main contribution to (2.1)-(2.2) is made by the terms $d_m = \tau_{ij}\varepsilon^p_{ij}$ and $d_T = -\mathbf{q}\cdot\mathrm{grad}\,T/T$. The last term is the capacity for heat dissipation and, in the case of the Fourier heat-conduction law $\mathbf{q} = -\kappa\,\mathrm{grad}\,T$, has the form $d_T = \kappa(\mathrm{grad}\,T)^2/T$.

3. Testing of the Model. To substantiate the model, we solved two-dimensional axisymmetric problems involving the normal collision of cylindrical grains with a rigid wall and a rigid cylindrical projection (Fig. 1a and b).

Since the characteristic time of the collision process is short (corresponding to the time required for several elastic wave propagations through the striker), the collision problem was solved in an adiabatic approximation (div $\mathbf{q} = 0$). We also ignored the strain anisotropy of the material, assuming that $\Gamma = 0$. In this case, the mass, momentum, and internal energy equations are written in the cylindrical coordinate system rz:

$$\begin{aligned}
&\frac{\dot{\rho}}{\rho} = -\dot{\varepsilon}_{rr} - \dot{\varepsilon}_{zz} - \dot{\varepsilon}_{\theta\theta},\\
&\rho\dot{v}_r = \frac{\partial\sigma}{\partial r} + \frac{\partial S_{rr}}{\partial r} + \frac{\partial S_{rz}}{\partial z} + \frac{S_{rr} - S_{\theta\theta}}{r},\\
&\rho\dot{v}_z = \frac{\partial\sigma}{\partial z} + \frac{\partial S_{zz}}{\partial z} + \frac{\partial S_{rz}}{\partial r} + \frac{S_{rz}}{r},\\
&\rho c_\sigma \dot{T} + \alpha_V \sigma \dot{T} = S_{rr}\dot{\varepsilon}^p_{rr} + S_{zz}\dot{\varepsilon}^p_{zz} + S_{\theta\theta}\dot{\varepsilon}^p_{\theta\theta}\\
&+ 2S_{rz}\dot{\varepsilon}^p_{rz} + A\dot{\alpha}^2.
\end{aligned} \tag{3.1}$$

We write the expressions for the strain rates as

$$\dot{\varepsilon}_{rr} = \frac{\partial v_r}{\partial r},\quad \dot{\varepsilon}_{zz} = \frac{\partial v_z}{\partial z},\quad \dot{\varepsilon}_{\theta\theta} = \frac{v_r}{r},\quad \dot{\varepsilon}_{rz} = \frac{1}{2}\left(\frac{\partial v_r}{\partial z} + \frac{\partial v_z}{\partial r}\right) \tag{3.2}$$

(v_r, v_z are projections of the velocity vector on the r and z axes).

The initial conditions at t = 0:

$$v_r = 0,\ v_z = -V_0,\ \rho = \rho_0,\ \sigma = S_{ij} = 0$$

(V_0 is initial collision velocity).

The boundary conditions: $\sigma_{ij}n_j = 0$ on the free surface of the striker (n_j represents components of a unit formal to the outside surface of the striker); $v_z = 0$ and $\sigma_{rz} = 0$ on the part $\Sigma(t)$ of the surface of the striker in contact with the target ($\Sigma(t)$ and the free surface of the striker are determined in the course of the solution of the problem). Also, it is assumed that the striker moves along the surface of the target without friction.

We determine the moment the striker rebounds from the target by using the criterion of vanishing of their forces of interaction [21, 22]:

$$F(t) = -\int\limits_{\Sigma(t)}\int \sigma_{zz}dz. \tag{3.3}$$

The collision problem was solved numerically on a Lagrangian grid in accordance with an explicit finite-difference scheme of the type described in [18]. The calculations were performed for solid VRA fuel with ρ_0 = 1850 kg/m, K_0 = 5.666 GPa, μ_0 = 1.244 GPa, Y = 0.0866 GPa, $\alpha_V = 3\cdot10^{-6}$ K^{-1}, c_σ = 1.23 kJ/(kg·K), T_m = 1000 K. Absolute viscosity η = 10 Pa·sec, which is typical of reactive solids [16]. The initial temperature T_0 = 300 K. The gas filling the micropores was air under normal conditions: P_0 = 0.1 MPa, k = 1.4. We took A = $5\cdot10^3$ Pa·sec as the parameter linking the processes of deformation and evolution of the micropores. This value was obtained as follows. We numerically solved the problem of the dynamic compression of a micropore of an initial external radius b_0 and internal radius a_0. The pore contained a gas or was hollow and was subjected to an external pressure pulse P = P(t) that was uniformly distributed over the outside surface of the cell. The duration of the pulse was τ [17]. Here, we determined the mean-mass temperature of the cell at the moment of unloading

$$\langle T\rangle = \int\limits_a^b 4\pi r^2\rho T dr \Big/ \int\limits_a^b 4\pi r^2\rho dr$$

for a "porous" cell ($a_0 \neq 0$) $-\overset{\circ}{\langle T\rangle}$ and a "solid" cell ($a_0 = 0$) $-\langle\overset{\circ}{T}\rangle$. We thus found the temperature increment $\Delta\langle T\rangle - \langle T\rangle$ due to the "porosity" of the cell. The problem on micropore dynamics was cast in a unidimensional formulation with allowance for its spherical symmetry. The gas was assumed to be ideal and the process adiabatic. We used equations of thermoelastoviscoplasticity of the Pezhina type [23] as the constitutive equations for the material of the pores. We took the same absolute viscosity η as in kinetic equation (1.2). We then numerically solved the problem of the plane collision of an aluminum plate and the test material, with the porosity $\alpha_0 = a_0^3/b_0^3$ and $\alpha_0 = 0$ in thermoelastoplastic approximation (1.1). This collision took place at the velocity V_0. The problem of plane collision has been examined in [11, 19], among other studies. The collision velocity V_0 and the thickness H of the striker were chosen so as to ensure a pressure on the order of P with a duration τ in the frontal layer of the target. By varying the parameter A of model (1.1), we were able to find a value of A which ensured that the amount by which the temperature in the frontal layer of the porous target exceeded the same temperature in the solid target ($\alpha_0 = 0$) was the same as in the problem of an isolated pore. Calculations were performed for different b_0, α_0, P, and τ. Here, we succeeded in finding a value of A which satisfactorily described all of the calculations.

Figures 2-6 show some of the calculated results obtained for $V_0 = 200$ m/sec and $\alpha_0 = 0.1$. Figure 2 shows the relations for the dimensionless force of interaction $F(t)/mg$ of the strikers and the targets for cases a and b in Fig. 1 (mg is the weight of the striker, $\bar{t} = tc_0/H$ is dimensionless time, $c_0 = \sqrt{(K_0 + (3/4)/\mu_0)/\rho_0}$ is the speed of sound). Figure 3 shows lines depicting the level of porosity α, while Fig. 4 shows increments of temperature ΔT (the numbers on the left) and dissipation D (the numbers on the right) at the moment the striker rebounds from the flat wall. Figure 5 shows lines illustrating the level of porosity α and Fig. 6 shows increments of temperature ΔT (the numbers on the left) and dissipation (the numbers on the right) at the moment the striker rebounds from the wall with the projection.

If follows from the calculations that the interaction of the strikers and the targets is distinctly wavelike in character. A compression wave with a two-wave configuration is formed at the striker–target contact surface at the beginning of the collision process, with the velocities of the components of this wave differing substantially. The first wave is elastic, while the second wave is plastic. The amplitude and velocity of the latter depend on collision velocity. Unloading waves propagating from the lateral surfaces of the strikers that are free of loads reduce the intensity of the loading waves and distort the initially plane compression front. Thus, the stress–strain state of the strikers differs appreciably from the stress–strain state calculated in a unidimensional approximation (uniaxial stress state (rod approximation) or uniaxial strain state (thin-plate approximation)). Having reached the free back surface of the striker, the elastic wave is reflected from the free surface as an unloading wave and moves counter to the front of the plastic compression wave. Their interaction results in a decrease in the intensity of the plastic wave, while the elastic compression wave again propogates toward the free back surface. The process just described continues until the amplitude of unloading waves (both from the back surface and from the lateral surface) equals the amplitude of the plastic compression wave. The stresses ultimately become tensile, which causes the striker to rebound from the target. The free lateral surface causes contact with the points of the striking end to be lost at different moments of time. This is particularly evident from Fig. 2. After the elapse of a certain period of time, contact is restored at these points on the surface of the target. This matter was examined in [22] for the case of the impact of a prismatic rod against a rigid wall.

In the case of the impact of a cylinder against a wall with a projection, the interaction process is quite nonuniform from the very first moments of the collision process. The first abrupt increase in the interaction force (line b in Fig. 2) is connected with the impact of the main part of the front surface of the cylinder on the target. The graph of this force is subsequently similar to the graph of the force F(t) in the case of collision with a wall without a projection (Fig. 2, line a). The durations of the interactions for these two cases are markedly different, which can be attributed to the effect of the projection.

We should point out that the given material is less affected than metals by the so-called intermediate rebound phenomenon (here, the force of interaction F(t) vanishes before the beginning of the final rebound of the striker from the target). In the case of metals,

this phenomenon is seen both for long strikers (intermediate rebound at the final stage of interaction) and (to a greater extent) for short strikers (intermediate rebound in the middle of the interaction process) [22, 24]. This is probably related to the high degree of compressibility of the fuel – including the compressibility due to the presence of micropores.

The character of distribution of lines depicting the levels of the increments of temperature ΔT and dissipation D is the same. The nonuniformity of the fields of ΔT and D depends on the characteristic deformation zones. The zones of elevated temperature at the free ends of the strikers are connected with the wave character of the deformation process (rapid tension of the material at the sites of collision of counter-directed unloading waves propogating from the front and back surfaces of the striker). The largest increase in temperature in the case of collision with the flat wall is seen near the front surface at the periphery of the striker. In the case of impact against the wall with the projection, the greatest energy dissipation occurs near the projection in an annular region whose radius is roughtly equal to the radius of the cavity created by the projection. Failure of the material should also be expected in these regions of increased energy dissipation.

Plastic flow of pores occurs near the striker–target contact surface, while pore growth takes place near the back surface. There are sizable regions (the hatched regions in Figs. 3 and 5) in which porosity remains constant. This phenomenon was noted in [25].

Thus, we have constructed a coupled model of a porous thermoelastoplastic body. A failure criterion based on the limiting unit dissipation was proposed. In principle, this criterion makes it possible to describe failure in a complex stress state either by the shear mechanism or by the tensile mechanism, reflecting an increase in the porosity of the material. Plastic flow of pores occurs in the compression zones. The change in porosity in turn has an effect on the stress state of the material and is accompanied by energy dissipation. The model accounts for the presence of gas in the pores. With the use of the solution of problems involving the collision of cylindrical specimens with solid targets as an example, it was shown that the model correctly describes the main features of the process, while the failure criterion makes it possible to predict the locations of the regions of macroscopic failure.

LITERATURE CITED

1. R. Nev'er, M. Nait-Abdelaznz, and G. Plyuvanazh, "Method of studying defects in solid rocket fuels," Probl. Prochn., No. 3 (1989).
2. L. M. Kachanov, "Time to failure under creep conditions," Izv. Akad. Nauk SSSR Otd. Tekh. Nauk, No. 8 (1958).
3. Yu. N. Rabotnov, Creep of Structural Elements [in Russian], Nauka, Moscow (1966).
4. A. A. Il'yushin, "Theory of rupture strength," Inzh. Zh. Mekh. Tverd. Tela, No. 3 (1967).
5. O. V. Sosnin, "Variant of creep theory with energy-based strain-hardening parameters," in: Mechanics of Deformable Bodies and Structures [in Russian], Mashinostroenie, Moscow (1975).
6. V. S. Nikiforovskii and E. I. Shemyakin, Dynamic Failure of Solids [in Russian], Nauka, Novosibirsk (1979).
7. S. A. Shesterikov and A. M. Lokoshchenko, "Creep and rupture strength of metals," Itogi Nauki Tekh. Ser. Mekh. Deform. Tverd. Tela, 13 (1980).
8. V. V. Bolotin, "Generalized models in fracture mechanics," Izv. Akad. Nauk SSSR, Mekh. Tverd. Tela, No. 3 (1984).
9. V. N. Kukudzhanov, "Numerical modeling of the unsteady deformation and fracture of elastoplastic bodies with large strains," in: Mathematical Methods in the Mechanics of Deformable Solids [in Russian], Nauka, Moscow (1986).
10. V. I. Kondaurov and L. V. Nikitin, Principles of the Rheology of Geologic Materials [in Russian], Nauka, Moscow (1990).
11. A. B. Kiselev and M. V. Yumashev, "Deformation and fracture during impact loading. Model of a damaged thermoelastoplastic medium," Prikl. Mekh. Tekh. Fiz., No. 5, (1990).
12. I. Prigozhin, Introduction to the Thermodynamics of Irreversible Processes [in Russian], IL, Moscow (1960).
13. V. G. Grigor'ev, S. Z. Dunin, and V. V. Surkov, "Collapse of a spherical pore in a viscoplastic material," Izv. Akad. Nauk SSSR Mekh. Tverd. Tela, No. 1 (1981).
14. V. K. Golubev, "Expansion of pores in ductile metals during cleavage," Prikl. Mekh. Tekh. Fiz., No. 6 (1983).

15. Sh. U. Galiev, Nonlinear Waves in Finite Continua [in Russian], Naukova Dumka, Kiev (1988).
16. V. V. Selivanov, V. S. Solov'ev, and N. N. Sysoev, Shock and Detonation Waves. Methods of Investigation [in Russian], Izd. MGU, Moscow (1990).
17. A. B. Kiselev and M. V. Yumashev, "Numerical study of the shock compression of a micropore in a thermoelastoviscoplastic material," Vestn. Mosk. Univ. Mat. Mekh., No. 1 (1992).
18. M. L. Wilkins, "Modelling the behavior of materials," Struct. Impact and Crashworthiness. Proc. Int. Conf., Vol. 2, London; New York (1984).
19. A. B. Kiselev and M. V. Yumashev, "Criteria of the dynamic failure of a thermoelastoplastic medium," Vestn. Mosk. Univ. Mat. Mekh., No. 4 (1990).
20. B. E. Pobedrya, "Fracture criteria of structurally nonuniform materials," in: Plastic Deformation and Fracture of Solids [in Russian], Nauka, Moscow (1988).
21. A. I. Gulidov and V. M. Fomin, "Numerical modelling of the rebound of axisymmetric rods from a solid barrier," Prikl. Mekh. Tekh. Fiz., No. 3 (1980).
22. A. B. Kiselev, "Numerical study, in a three-dimensional formulation, of the collision of elastoplastic bodies with a rigid barrier," Vestn. Mosk. Univ. Mat. Mekh., No. 4 (1985).
23. P. Pezhina, Basic Principles of Viscoplasticity, [Russian translation], Mir, Moscow (1968).
24. V. M. Boiko, A. I. Gulidov, A. I. Papyrin, et al., "Experimental-theoretical study of the rebound of short rods from a solid barrier," Prikl. Mekh. Tekh. Fiz., No. 5, (1982).
25. S. P. Kiselev, V. M. Fomin, and Yu. A. Shitov, "Numerical modelling of the rebound of a porous cylinder from a rigid barrier," Prikl. Mekh. Tekh. Fiz., No. 3 (1990).

LAWS OF THE KINETIC THEORY OF STRENGTH OF FROZEN SOILS

A. A. Konovalov

UDC 624.139

The studies [1, 2], devoted to the rheology of frozen soils, demonstrated the kinetic nature of the strength of these soils and presented a physical interpretation of the parameters of an equation describing their long-term strength from an atomic-kinetic viewpoint. However, these findings have not found expression in the mathematical theory of the rheology of frozen soils. Nor has use been made of quantitative relations and parameters expressing the temperature-time dependence of strength. According to [3] such relations and parameters can be established for all solids. Standard interpolation formulas which include empirical coefficients serve as the basis of quantitative methods of determining the strength characteristics of frozen soil. In particular, use is made of the coefficient [1]:

$$\tau = (g/\sigma)^{1/\Gamma}. \tag{1}$$

Here, τ is the time to failure (life); σ is pressure; g and Γ are empirical coefficients dependent on temperature, soil composition, type of load, etc.

We will attempt to find the temperature dependence of the strength of frozen soil in explicit form. Equation (1) is conveniently represented as

$$\tau = \tau_0(\sigma_m/\sigma)^{1/\Gamma}, \tag{2}$$

where σ_m is the instantaneous (maximum) strength corresponding to the minimum life ("moment") τ_0. In accordance with the representations of atomic-kinetic theory, this physical "moment" is equal to the period of thermal vibration of the atoms $\tau_0 \approx 10^{-13}$ sec.

Tyumen'. Translated from Prikladnaya Mekhanika i Tekhnicheskaya Fizika, No. 6, pp. 134-139, November-December, 1992. Original article submitted June 24, 1991.

 0021-8944/92/3306-0892$12.50